ELSEVIER

Contents lists available at ScienceDirect

Results in Chemistry

journal homepage: www.sciencedirect.com/journal/results-in-chemistry





Analytical concentration impedance of a transport layer

Andrei Kulikovsky 1

Forschungszentrum Jülich GmbH, Theory and Computation of Energy Materials (IEK-13), Institute of Energy and Climate Research, D-52425 Jülich, Germany

ARTICLE INFO

Keyword: Concentration impedance cFRA Transport layer impedance EPIS

ABSTRACT

A formula for concentration (zeta-) impedance of reactant transport through a finite–length layer attached to the electrochemical electrode is derived. The static point of the Nyquist spectrum is independent of the layer transport parameters, while the peak of $-\Im\zeta$ is located at the frequency which is close to the Warburg finite–length frequency.

1. Introduction

Electrochemical impedance spectroscopy (EIS) is a unique noninvasive, operando tool for fuel cells testing and characterization. Interpretation of impedance spectra could be done using either physics-based modeling (see reviews [1,2]), or distribution of relaxation times (DRT) [3,4]. However, physics-based modeling is a complicated tool, while DRT fails to separate the processes with close characteristic frequencies.

To overcome this limitation, in recent years an alternative impedance techniques have been investigated [5–9]. Due to oxygen reduction reaction (ORR), current, potential and oxygen concentration in a polymer electrolyte membrane (PEM) fuel cell are tightly coupled and small perturbation of any of the three variables induces linear response of the other two. In particular, one may perturb the oxygen concentration δc and measure the respective perturbation of the cell potential δV . Below, the ratio $\zeta = \delta V/\delta c$ will be referred to as the concentration impedance, or zeta–impedance. Analysis shows that zeta–impedance is independent of faradaic processes in the cell [10]. This makes zeta–spectroscopy a viable complementary to EIS technique, especially in cases when one of the oxygen transport processes overlaps with the faradaic reaction on the frequency scale.

A classic solution for electric impedance of a semi-infinite transport layer (TL) has been derived by Warburg [11]. Later, his approach has been applied to obtain impedance of a finite—length TL [12]. In [10], a model for the concentration impedance of the gas diffusion and cathode catalyst layers in PEM fuel cell has been developed assuming large stoichiometry of the air flow and large oxygen consumption in the catalyst layer. (See Table 1).

From theoretical standpoint, it is of large interest to derive solution

for zeta-impedance of a finite-length TL operating in standard conditions. This seems to be a simplest, refined formulation of zeta-impedance problem. Below, we develop a model for zeta-impedance of the TL. The model leads to analytical formula for the zeta-impedance.

2. Model

To bring the model closer to experiment, suppose that the transport layer is located between the air channel and the cathode catalyst layer (CCL) in a PEM fuel cell (Fig. 1). Our goal is analytical formula for the TL concentration impedance.

The model is based on the following assumptions.

- The dominating mechanism of oxygen transport through the TL is diffusion
- Oxygen and proton transport in the CCL are fast
- The electrode operates under fixed current density

The second assumption allows us to simplify the electrode model; below, it is shown that TL concentration impedance depends on the electrode properties, much like the corrected Warburg impedance [13]. The last assumption means that the electronic equipment blocks oscillations of the cell current density. This condition is typical for EPIS experiments [6–9].

Oxygen transport in the TL is thus described by the transient diffusion equation

$$\frac{\partial c_b}{\partial t} - D_b \frac{\partial^2 c_b}{\partial x^2} = 0, \quad D_b \frac{\partial c_b}{\partial x} \Big|_{x=l_t} = \frac{j_0}{4F}, \quad c_b \left(l_t + l_b \right) = c_h, \tag{1}$$

where c_b is the oxygen concentration in the TL, t is time, x is the distance

E-mail address: A.Kulikovsky@fz-juelich.de.

Also at: Lomonosov Moscow State University, Research Computing Center, 119991 Moscow, Russia

Nomenclature		R	Gas constant
		R_{TL}	Concentration "resistivity" of the TL, V cm ³ mol ⁻¹ , Eq.(24)
\sim	Marks dimensionless variables	t	Time, s
b	ORR Tafel slope, positive by convention, V	t*	Characteristic time, s, Eq.(5)
C_{dl}	Double layer volumetric capacitance, F cm ⁻³	x	Coordinate through the cell, cm
c	Oxygen molar concentration in the CCL, mol cm ⁻³		
c_b	Oxygen molar concentration in the TL, mol cm^{-3}	Subscripts:	
c_h	Oxygen molar concentration in the channel, mol cm ⁻³	0	Membrane/CCL interface
c_{ref}	Reference (inlet) oxygen concentration, mol cm ⁻³	1	CCL/TL interface
D_b	Oxygen diffusion coefficient in the TL, $cm^2 s^{-1}$	b	In the TL
F	Faraday constant, C mol ⁻¹	Superscripts	
f	Frequency, Hz	0	Steady–state value
f_W	Warburg finite-length frequency, Hz, Eq.(25)	1	Small-amplitude perturbation
i*	ORR volumetric exchange current density, A cm ⁻³		
i	Imaginary unit	Greek:	
j	Local proton current density in the CCL, A cm ⁻²	η	ORR overpotential, positive by convention, V
j_0	Cell current density, A cm ⁻²	ζ	Concentration impedance, V cm ³ mol ⁻¹ , Eq.(20)
l_b	TL thickness, cm	μ	Dimensionless parameter, Eq.(8)
l_t	CCL thickness, cm	ω	Angular frequency of the AC signal, s^{-1}

Table 1The standard PEM fuel cell parameters [16] used in calculations.

Transport layer thickness l_b , cm	0.025
Catalyst layer thickness l_t , cm	$10^{-3} (10 \mu m)$
Transport layer oxygen diffusivity D_b , cm ² s ⁻¹	0.02
ORR Tafel slope b, V	0.03
Double layer capacitance C_{dl} , F cm ⁻³	20
Cell current density j_0 , A cm ⁻²	0.1
Pressure, atm	1.0
Cell temperature T, K	$273\ +80$

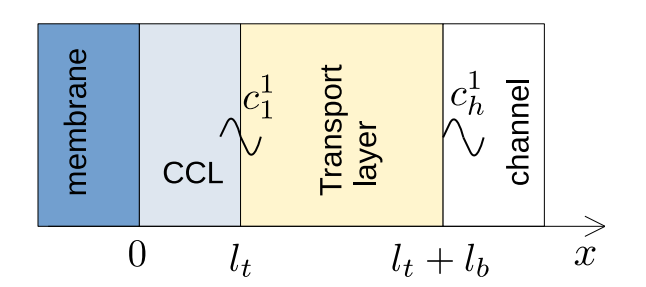


Fig. 1. Schematic of a transport layer considered in this work. CCL stands for the cathode catalyst layer, c_h^1 and c_1^1 are the oxygen concentration perturbations (see below).

through the system counted from the membrane (Fig. 1), D_b is the oxygen diffusion coefficient, l_t is the CCL thickness, l_b is the TL thickness, and j_0 is the current density in the electrode. The left boundary condition for Eq.(1) means that the oxygen flux in the TL obeys to stoichiometric requirement, and the right boundary condition fixes the channel oxygen concentration c_h at the TL/channel interface ($x = l_t + l_b$).

Current and overpotential in the electrode are related by the proton charge conservation equation (Ref.[14], page 313)

$$C_{dl}\frac{\partial \eta}{\partial t} + \frac{\partial j}{\partial x} = -i_* \left(\frac{c}{c_{ref}}\right) \exp\left(\frac{\eta}{b}\right)$$
 (2)

where C_{dl} is the double layer capacitance, η is the positive by convention ORR overpotential, j is the local proton current density, i_* is the ORR volumetric exchange current density (A cm $^{-3}$), c is the oxygen concentration in the electrode, c_{ref} is the reference oxygen concentration, and b is the ORR Tafel slope. The first term on the left side of Eq.(2) describes

charging/discharging of the double layer capacitance, which is assumed to be uniformly distributed over the CCL volume. The right side of Eq.(2) represents the Tafel rate of proton consumption in the ORR.

Assumption of fast proton and oxygen transport in the CCL means that η and c are nearly independent of x. Small variation of η along x is provided by large proton conductivity, so that the proton current $j=-\sigma_p\partial\eta/\partial x$ remains finite. Integrating Eq.(2) over x from zero to l_t , we get

$$C_{dl}l_{t}\frac{\partial\eta_{0}}{\partial t}-j_{0}=-i_{*}l_{t}\left(\frac{c_{1}}{c_{ref}}\right)\exp\left(\frac{\eta_{0}}{b}\right) \tag{3}$$

where η_0 is the ORR overpotential at x=0 and c_1 is the oxygen concentration at the CCL/TL interface. Note that the product $C_{dl}l_t$ (F cm⁻²) can be considered as a superficial double layer capacitance of the electrode.

It is convenient to introduce dimensionless variables

$$\widetilde{t} = \frac{t}{t_*}, \quad \widetilde{x} = \frac{x}{l_t}, \quad \widetilde{c} = \frac{c}{c_{ref}},$$

$$\widetilde{j} = \frac{j}{i_* l_t}, \quad \widetilde{\eta} = \frac{\eta}{b}, \quad \widetilde{D}_b = \frac{4FD_b c_{ref}}{i_* l_t^2}, \quad \widetilde{l}_b = \frac{l_b}{l_t}, \quad \widetilde{\omega} = \omega t_*, \quad \widetilde{\zeta} = \frac{\zeta c_{ref}}{b}$$
(4)

where the time scale t_* is

$$t_* = \frac{C_{dl}b}{i_*},\tag{5}$$

 ω is the angular frequency of the applied AC signal, and ζ is the concentration impedance (see below). With these variables, Eqs.(1), (3) read

$$\mu^{2} \frac{\partial \widetilde{c}_{b}}{\partial \widetilde{t}} - \widetilde{D}_{b} \frac{\partial^{2} \widetilde{c}_{b}}{\partial \widetilde{x}^{2}} = 0, \quad \widetilde{D}_{b} \frac{\partial \widetilde{c}_{b}}{\partial \widetilde{x}} \bigg|_{\widetilde{x}=1} = \widetilde{j}_{0}, \quad \widetilde{c}_{b} \left(1 + \widetilde{l}_{b} \right) = \widetilde{c}_{h}, \tag{6}$$

$$\frac{\partial \widetilde{\eta}_0}{\partial \widetilde{t}} - \widetilde{j}_0 = -\widetilde{c}_1 \exp \widetilde{\eta}_0 \tag{7}$$

where μ is the dimensionless parameter

$$\mu = \sqrt{\frac{4Fc_{ref}}{C_{tib}}} \tag{8}$$

Linearization and Fourier-transform of Eqs.(6), (7) is performed using the following expansions

$$\widetilde{c}_{b}(\widetilde{x},\widetilde{t}) = \widetilde{c}_{b}^{0}(\widetilde{x}) + \widetilde{c}_{b}^{1}(\widetilde{x},\widetilde{\omega}) \exp(i\widetilde{\omega}\widetilde{t}) \quad \widetilde{c}_{b}^{1} \ll \widetilde{c}_{b}^{0}
\widetilde{y}_{1}(\widetilde{t}) = \widetilde{y}_{1}^{0} + \widetilde{y}_{1}^{1}(\widetilde{\omega}) \exp(i\widetilde{\omega}\widetilde{t}) \quad \widetilde{y}_{1}^{1} \ll \widetilde{y}_{1}^{0}$$
(9)

where \widetilde{y}^1 stands for \widetilde{c}^1 , $\widetilde{\eta}^1$, \widetilde{j}^1 and the superscripts 0 and 1 mark the static variables and small perturbation amplitudes, respectively. This leads to the system of linear equations for the perturbation amplitudes $\widetilde{\eta}^1$, \widetilde{c}_b^1 and \widetilde{j}^1 in the $\widetilde{\omega}$ -space [15]

$$\widetilde{D}_{b} \frac{\partial^{2} \widetilde{c}_{b}^{1}}{\partial \widetilde{x}^{2}} = i\widetilde{\omega} \mu^{2} \widetilde{c}_{b}^{1}, \quad \widetilde{D}_{b} \frac{\partial \widetilde{c}_{b}^{1}}{\partial \widetilde{x}} \Big|_{\widetilde{c}=1} = \widetilde{j}^{1}, \quad \widetilde{c}_{b}^{1} \left(1 + \widetilde{l}_{b} \right) = \widetilde{c}_{h}^{1}, \tag{10}$$

$$\widetilde{j}^{1} = i\widetilde{\omega}\widetilde{\eta}^{1} + e^{\widetilde{\eta}_{0}} \left(\widetilde{c}_{1}^{1} + \widetilde{c}_{1}^{0}\widetilde{\eta}^{1} \right), \tag{11}$$

where \widetilde{c}_b^1 and \widetilde{c}_h^1 are the oxygen concentration perturbation amplitudes in the TL and channel, respectively, and \widetilde{c}_1^1 is this amplitude at the CCL/TL interface.

The Tafel law

$$\widetilde{j}_0 = \widetilde{c}_0^0 e^{\widetilde{\eta}_0} \tag{12}$$

allows us to eliminate $e^{\widetilde{\eta}_0}$ from Eq.(11) leading to

$$\widetilde{j}^{l} = i\widetilde{\omega}\widetilde{\eta}^{1} + \widetilde{j}_{0} \left(\frac{\widetilde{c}_{1}^{1}}{\widetilde{c}_{1}^{0}} + \widetilde{\eta}^{1} \right), \tag{13}$$

where \tilde{j}_0 is the static current density. Solving Eq.(10) and substituting $\tilde{x} = 1$ into the solution, we find the perturbation of oxygen concentration at the CCL/TL interface $\tilde{c}_b^1(1)$:

$$\widetilde{c}_{b}^{1}\left(1\right) = -\frac{\widetilde{j}^{1}\tanh\left(q\widetilde{l}_{b}\right)}{q\widetilde{D}_{b}} + \frac{\widetilde{c}_{h}^{1}}{\cosh\left(q\widetilde{l}_{b}\right)}.$$
(14)

where

$$q = \mu \sqrt{\frac{i\widetilde{\omega}}{\widetilde{D}_{h}}}.$$
 (15)

Continuity of the oxygen concentration prescribes that $\tilde{c}_b^1(1) = \tilde{c}_1^1$. Substituting \tilde{j}^1 from Eq.(13) into Eq.(14), equating Eq.(14) to \tilde{c}_1^1 and solving the resulting equation for \tilde{c}_1^1 , we come to

$$\widetilde{\boldsymbol{c}}_{1}^{1} = -\frac{\widetilde{\boldsymbol{\eta}}^{1} \mathrm{tanh} \Big(\boldsymbol{q} \widetilde{\boldsymbol{l}}_{b} \Big) \Big(\widetilde{\boldsymbol{j}}_{0} + \mathrm{i} \widetilde{\boldsymbol{\omega}} \Big)}{\mu \sqrt{\mathrm{i} \widetilde{\boldsymbol{\omega}} \widetilde{\boldsymbol{D}}_{b}} + \widetilde{\boldsymbol{j}}_{0} \mathrm{tanh} \Big(\boldsymbol{q} \widetilde{\boldsymbol{l}}_{b} \Big) \bigg/ \widetilde{\boldsymbol{c}}_{1}^{0}} + \frac{\widetilde{\boldsymbol{c}}_{b}^{1} \mu \sqrt{\mathrm{i} \widetilde{\boldsymbol{\omega}} \widetilde{\boldsymbol{D}}_{b}}}{\mu \sqrt{\mathrm{i} \widetilde{\boldsymbol{\omega}} \widetilde{\boldsymbol{D}}_{b}} \mathrm{cosh} \Big(\boldsymbol{q} \widetilde{\boldsymbol{l}}_{b} \Big) + \widetilde{\boldsymbol{j}}_{0} \mathrm{sinh} \Big(\boldsymbol{q} \widetilde{\boldsymbol{l}}_{b} \Big) \bigg/ \widetilde{\boldsymbol{c}}_{1}^{0}}.$$

3. Results and discussion

Eq.(16) relates the three perturbation amplitudes: oxygen concentration at the CCL/TL interface \widetilde{c}_1^1 , overpotential $\widetilde{\eta}^1$, and oxygen concentration in the channel \widetilde{c}_h^1 (Fig. 1). Of these three amplitudes, \widetilde{c}_h^1 is the applied one, $\widetilde{\eta}^1$ is the measured one, while \widetilde{c}_1^1 is unknown and it could hardly be measured. The latter amplitude makes the problem of theoretical description of ζ -impedance "as is" under-determined. However, if the perturbation of the total (external) current in the cell is kept zero,

the problem has a unique solution.

Fixed external current means that the perturbation of total current density (capacitive plus conductive) is zero:

$$i\widetilde{\omega}\widetilde{\eta}^1 - \widetilde{j}^1 = 0 \tag{17}$$

With this, Eq.(13) simplifies to

$$0 = \frac{\widetilde{c}_1^1}{\widetilde{c}_1^0} + \widetilde{\eta}^1. \tag{18}$$

Using Eq.(17), Eq.(14) takes the form

$$\widetilde{c}_{b}^{1}\left(1\right) = -\frac{\mathrm{i}\widetilde{\omega}\widetilde{\eta}^{1}\tanh\left(\widetilde{q}\widetilde{l}_{b}\right)}{\widetilde{q}\widetilde{D}_{b}} + \frac{\widetilde{c}_{b}^{1}}{\cosh\left(\widetilde{q}\widetilde{l}_{b}\right)}.$$
(19)

Substituting $\tilde{c}_1^1 = \tilde{c}_b^1(1)$ into Eq.(18), dividing the resulting equation by \tilde{c}_b^1 and solving for

$$\widetilde{\zeta} = -\frac{\widetilde{\eta}^1}{\widetilde{c}_h^1} \tag{20}$$

we finally get

$$\widetilde{\zeta} = -\left(\cosh\left(\mu \widetilde{l}_b \sqrt{\mathrm{i}\widetilde{\omega}/\widetilde{D}_b}\right) \left(\frac{\mathrm{i}\widetilde{\omega} \tanh\left(\mu \widetilde{l}_b \sqrt{\mathrm{i}\widetilde{\omega}/\widetilde{D}_b}\right)}{\mu \widetilde{D}_b \sqrt{\mathrm{i}\widetilde{\omega}/\widetilde{D}_b}} - \widetilde{c}_1^0\right)\right)^{-1} \tag{21}$$

The minus sign in Eq.(20) is taken as the variations of cell potential and $\tilde{\eta}^1$ have opposite signs. Taking into account that

$$\widetilde{c}_{1}^{0} = 1 - \frac{j_{0}}{j_{\lim}}, \quad j_{\lim} = \frac{4FD_{b}c_{ref}}{l_{b}},$$
(22)

in the dimension form Eq.(21) reads

$$\zeta = \frac{4Fb\sqrt{\mathrm{i}\omega D_b}}{4Fc_{ref}(1 - j_0/j_{\mathrm{lim}})\sqrt{\mathrm{i}\omega D_b}\mathrm{cosh}\left(l_b\sqrt{\mathrm{i}\omega/D_b}\right) - \mathrm{i}\omega C_{dl}bl_t\mathrm{sinh}\left(l_b\sqrt{\mathrm{i}\omega/D_b}\right)}$$
(23)

Eq.(23) is a concentration impedance analog to the Warburg finite–length electric impedance of a transport layer. Dividing ζ by RT one gets the pressure impedance $\zeta_{V/P} = \zeta/(RT)$.

The spectra of Eq.(23) for the two indicated oxygen diffusion coefficients D_b in the TL are depicted in Fig. 2. As can be seen, in the Nyquist coordinates the two spectra do not differ. Indeed, the static point R_{TL} of the curl in Fig. 2a is independent of the TL transport

(16)

$$R_{TL} = \frac{b}{c_1^0}. (24)$$

However, the frequency dependence of imaginary part of ζ has a peak and a valley (Fig. 2b) with the peak frequency proportional to D_b . The peak frequency $f_{\rm max}$ is close to the Warburg finite–length frequency

$$f_{\text{max}} = \frac{2.39D_b}{2\pi l_b^2} \tag{25}$$

10-2

 10^{-1}

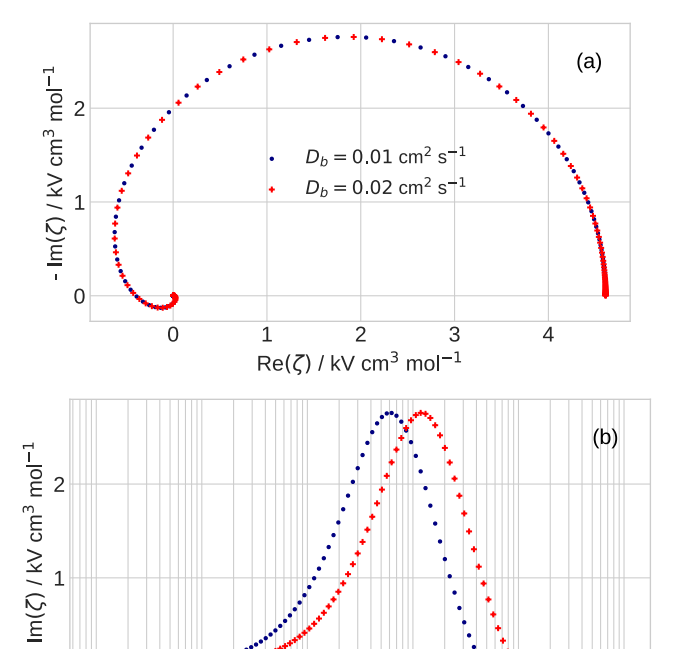


Fig. 2. (a) Nyquist spectrum of the transport layer concentration impedance, Eq.(23), for the indicated oxygen diffusion coefficients. (b) Frequency dependence of imaginary part of impedance in (a). Parameters for calculations are listed in Table 1.

frequency / Hz

 10^{2}

 10^{3}

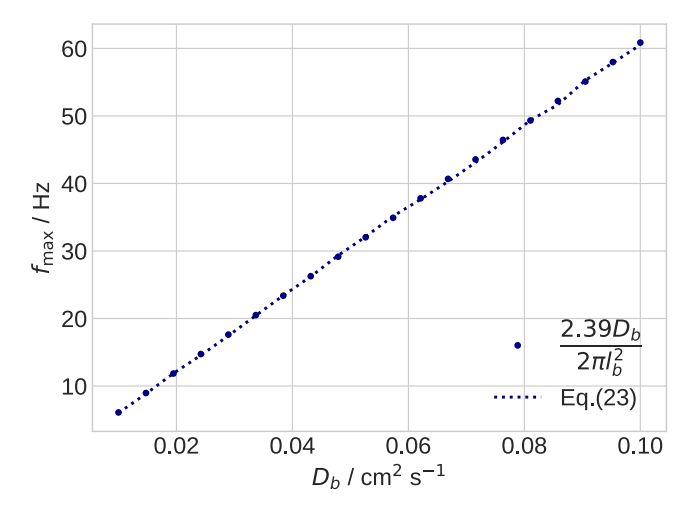


Fig. 3. Frequency of the peak of $-I(\zeta)$, Eq.(23), dotted line) and Warburg-like finite–length frequency, Eq.(25), points) vs oxygen diffusion coefficient D_b .

(Fig. 3), where the numeric coefficient is 2.39, while in the Warburg finite–length formula this coefficient is 2.54.

4. Conclusions

A model for concentration impedance ζ of a finite thickness transport

layer is developed and analytical solution for ζ is derived. The static value of ζ is independent of the layer transport parameters; however, the imaginary part $-I(\zeta)$ has a peak at the frequency close to the Warburg finite–length frequency.

Declaration of Competing Interest

The authors declare that they have no known competing financial interests or personal relationships that could have appeared to influence the work reported in this paper.

References

- [1] Z. Tang, Q.-A. Huang, Y.-J. Wang, F. Zhang, W. Li, A. Li, L. Zhang, J. Zhang, Recent progress in the use of electrochemical impedance spectroscopy for the measurement, monitoring, diagnosis and optimization of proton exchange membrane fuel cell performance, J. Power Sources 468 (2020), 228361, https:// doi.org/10.1016/j.jpowsour.2020.228361.
- [2] J. Huang, Y. Gao, J. Luo, S. Wang, C. Li, S. Chen, J. Zhang, Editors' choice–review–impedance response of porous electrodes: Theoretical framework, physical models and applications, J. Electrochem. Soc. 167 (2020), 166503, https://doi.org/10.1149/1945-7111/abc655.
- [3] R. Fuoss, J. Kirkwood, Electrical properties of solids. viii. Dipole moments in polyvinyl chloride-diphenyl systems, J. Am. Chem. Soc. 63 (1941) 385–394, https://doi.org/10.1021/ja01847a013.
- [4] H. Schichlein, A.C. Müller, M. Voigts, A. Krügel, E. Ivers-Tiffée, Deconvolution of electrochemical impedance spectra for the identification of electrode reaction mechanisms in solid oxide fuel cells, J. Appl. Electrochem. 32 (2002) 875–882, https://doi.org/10.1023/A:1020599525160.
- [5] A.M. Niroumand, W. Merida, M. Eikerling, M. Saif, Pressure–voltage oscillations as a diagnostic tool for PEFC cathodes, Electrochem. Comm. 12 (2010) 122–124, https://doi.org/10.1016/j.elecom.2009.11.003.
- [6] E. Engebretsen, T.J. Mason, P.R. Shearing, G. Hinds, D.J.L. Brett, Electrochemical pressure impedance spectroscopy applied to the study of polymer electrolyte fuel cells, Electrochem. Comm. 75 (2017) 60–63, https://doi.org/10.1016/j. elecom.2016.12.014.
- [7] A. Sorrentino, T. Vidakovic-Koch, R. Hanke-Rauschenbach, K. Sundmacher, Concentration–alternating frequency response: A new method for studying polymer electrolyte membrane fuel cell dynamics, Electrochim. Acta 243 (2017) 53–64, https://doi.org/10.1016/j.electacta.2017.04.150.
- [8] A.V. Shirsath, S. Rael, C. Bonnet, L. Schiffer, W. Bessler, F. Lapicque, Electrochemical pressure impedance spectroscopy for investigation of mass transfer in polymer electrolyte membrane fuel cells, Current Opinion in Electrochem. 20 (2020) 82–87, https://doi.org/10.1016/j.coelec.2020.04.017.
- [9] Q. Zhang, H. Homayouni, B.D. Gates, M. Eikerling, A.M. Niroumand, Electrochemical pressure impedance spectroscopy for polymer electrolyte fuel cells via back-pressure control, J. Electrochem. Soc. 169 (2022), 044510, https://doi. org/10.1149/1945-7111/ac6326.
- [10] A. Kulikovsky, Analytical model for PEM fuel cell concentration impedance, J. Electroanal. Chem. 899 (2021), 115672, https://doi.org/10.1016/j. ielechem. 2021.115672
- [11] E. Warburg, Über das Verhalten sogenannter unpolarisirbarer Electroden gegen Wechselstrom, Ann. Physik und Chemie 67 (1899) 493–499, https://doi.org/ 10.1002/andp.18993030302.
- [12] A. Lasia, Electrochemical Impedance Spectroscopy and its Applications, Springer, New York. 2014.
- [13] A. Kulikovsky, Why impedance of the gas diffusion layer in a PEM fuel cell differs from the Warburg finite-length impedance? Electrochem. Comm. 84 (2017) 28–31, https://doi.org/10.1016/j.elecom.2017.09.014.
- [14] A.A. Kulikovsky, Analytical Modelling of Fuel Cells, 2nd Edition, Elsevier, Amsterdam, 2019.
- [15] A. Kulikovsky, Analytical impedance of two-layer oxygen transport media in a PEM fuel cell, Electrochem. Comm. 135 (2022), 107187, https://doi.org/10.1016/ j.elecom.2021.107187.
- [16] T. Reshetenko, A. Kulikovsky, PEM fuel cell characterization by means of the physical model for impedance spectra, J. Electrochem. Soc. 162 (2015) F627–F633, https://doi.org/10.1149/2.1141506jes.